

Phytochemical fabrication of Silver nanoparticles using *Camellia sinensis* to probe their biological efficacy

Sudhakar T.¹, Lakshmipathy M.^{2*}, Umashankar G.¹, Premkumar J.¹, Roshan Sapkota¹,

Rijal Sakar¹ and Balashanmugam P.³

1. Department of Biomedical Engineering, School of Bio and Chemical Engineering, Sathyabama Institute of Science and Technology (Deemed to be University), Jeppiaar Nagar, Raajiv Gandhi salai, Chennai, Tamil Nadu 600 119, INDIA

2. Department of Conservative Dentistry and Endodontics, Saveetha Dental College and Hospitals, Saveetha Institute of Medical and Technical Sciences, Chennai, Tamil Nadu 600 077, INDIA

3. CSIR – Central Leather Research Institute (CLRI), Adyar, Chennai, Tamil Nadu 600 020, INDIA

*mlakshmipathy@gmail.com

Abstract

*One of the most sought-after practices that determine the success of tiny technology relies on broad spectrum applications and environmental safety. A simple one-pot method was adopted to fabricate stable silver nanoparticles using *Camellia sinensis* leaf extract. The synergistic antimicrobial effect of AgNPs was evaluated upon amalgamation with PLGA nanofibre. Characterization studies were performed using UV vis-spectroscopy, X-ray diffraction (XRD), Fourier transform infrared spectroscopy (FTIR) and Scanning electron microscopy (SEM). The antibacterial effect of the synthesized NPs immobilized PLGA nanofibre (PAN) was evaluated using agar diffusion method. Nanoparticle synthesis could be achieved rapidly within 30 minutes of the reaction demonstrating a single absorbance peak at 421 nm (λ_{max}). XRD and SEM results showed that particles were crystalline and circular in shape with size < 40nm. Phytochemical reduction and capping of NPs could clearly be evidenced from FTIR studies.*

Antimicrobial susceptibility screening of AgNPs (5, 10, 20, 40 μ g) performed using clinical isolates (n = 6) showed significant growth inhibition at higher concentrations. Similarly, nanoparticulate efficacy of AgNPs-PLGA membrane in overcoming resistance was demonstrated using their corresponding resistant counterparts. They forecasted significant inhibition in growth against all the resistant strains (individual and consortia) at 30 μ g concentration at par with conventional antibiotics at a given concentration. Such prepared nanoparticles inducing potential antibacterial activity might be fine-tuned prior to surface modification and biocompatibility studies for broad spectrum therapeutic modalities.

Keywords: *Camellia sinensis*, Silver nanoparticles, PLGA, Antimicrobial effect, Wound healing.

Introduction

Nature's creations have always been an inspiration for mankind to explore its secret mysteries. In this mission of natural mimicking, the human race has competed enough to

decode the protocol but landed up developing a technology, thereby getting civilized in every attempt. This connectivity and competency have resulted in technological succession toward nanoscale engineering feat. The skilful practise of manoeuvring materials at atomic and molecular scale has instilled novel properties and are used for wider applications. Nanotechnological concepts remain viable since ancient times evidencing the invention of Lycurgus cup¹, preparation of corrosion-resistant Maya blue pigment² and design of Damascus steel sword³.

Beyond its limitations, they were also found to have their applications in ancient medicine (Ayurveda) in the form of Bhasmas, a form of nanomedicine. This was a life-saving innovation where the metal / mineral were mixed with an herbal extract for treating chronic disorders. The peculiarity of this preparation lies in removing the toxic effects of metals and transforming into biologically active nanoparticles, the Bhasmas⁴. Additionally, the cosmetics used in ancient era were formulated using naturally available oils, plant extract and water but the then Romans and Greeks prepared and used nanotechnology based cosmetic products.

On the contrary, the modernizing world of technology has witnessed several advancements and surprising discoveries in the areas of electronics, physics, chemistry and biology. However, there exist some impediments viz. increase in incidences of lifestyle-induced-illnesses, metabolic disorders and emergence of multidrug resistant pathogens posing a major threat across the globe which needs multidimensional approach to counterbalance the situation. In this line, nano-based strategies toward medicinal and clinical applications tend to showcase a ray of hope in taking the prophylactic modalities to the generation-next theranostics.

Nanoparticles possessing outstanding physico-chemical and optochemical properties with profound implications have been reported⁴. Generally, metal nanoparticles can be prepared by physical, chemical and biological methods. It is obvious that physical method remains one of the simplest ways of producing nanoparticles using mechanical force attributing to top-down or bottom-up approach. Moreover, the physical properties such as high pressure, energy and temperature remain the mainstay and expensive as well for synthesizing nanoparticles. The chemical approaches viz. chemical reduction, electrochemical techniques, lithography

and photochemical reduction are most widely used for producing nanoparticles.

Although they have control over the size and shape, there is a need for fine-tuning and formulation as far as the medical applications are concerned. Alongside, the use of toxic chemicals during synthesis could induce some toxicity in the course of the stabilization leading to adverse effects and ecological disturbances. So, there is a growing need for the development of an eco-friendly process on a par with physical and chemical route of nanoparticle synthesis⁵.

A variety of preparation routes have been reported for reducing bulk metal precursors to acquire unusual properties in their nano form⁶. The most challenging one is phytochemical route of synthesis where an active or consortia of metabolites gets involved in the reduction process. However, bio-synthesis of nanoparticles is regarded as safe, reliable, eco-friendly, cheap and an easy to scale-up technology; but the exact mechanism by which the nanoparticle size is being controlled, remains unclear.

Meanwhile, metal nanoparticles produced using microbes and plant extracts are considered stable and monodisperse once the physiochemical parameters (pH, temperature, reaction period and mixing ratio) are controlled thereof. Among the various bionanoparticles, phytochemical mediated ones using medicinal plants have been found to be pharmacologically active, possibly due to the adhesion of several bioactive metabolites⁷⁻⁹.

Camellia sinensis (*C. sinensis*), an evergreen shrub, belongs to the family Theaceae. Their plant parts especially the leaves and leaf buds have gained economic significance as a beverage and its profound use in medicinal purposes. Encouraging data upon tea (leaf extract) consumption have shown to prevent debilitating human ill-effects. The most important chemicals present in green tea with considerable physiological effects and pharmacological significance are the polyphenols and alkaloids having significant role in the prevention of cardiovascular diseases. It is also best studied because of its cancer chemo preventive and chemotherapeutic effects¹⁰.

In the present study, silver nanoparticles were synthesised from green tea extract i.e. *C. sinensis* and analysed for defined nano characteristics. These nanoparticles were amalgamated onto PLGA-nano fibres and their antimicrobial efficacy toward selected clinical strain(s) / consortia was investigated pertaining to wound healing property.

Material and Methods

Materials: Silver nitrate (AgNO_3 , 99.8% purity) was sourced from SRL Laboratories, India and Mueller-Hinton Agar (MHA) medium was purchased from HiMedia™ India Ltd. The bacterial strains used in this study were as follows: *Staphylococcus aureus* (*S. aureus*), *Klebsiella pneumoniae*

(*K. pneumoniae*), *Escherichia coli* (*E. coli*), *Pseudomonas aeruginosa* (*P. aeruginosa*), *Proteus mirabilis* (*P. mirabilis*), *Enterococcus faecalis* (*E. faecalis*) and their corresponding resistant strains were obtained from the Department of Microbiology, PGIBMS, University of Madras, India. All other chemicals used in this study were of analytical grade and used without further purification.

Collection and preparation of plant leaf extracts: The tea leaves were collected from Munnar (Lat. 10°05'21" N and Long. 77°03'35" E) in idukki district, Kerala during the month of November. The fresh leaves were carefully transported using vented polyethylene bags to the laboratory and washed with deionised water and surface sterilized using mercuric chloride (0.01% HgCl_2 , HiMedia™, India). Further, the leaves were washed in running tap water to remove the traces of mercury.

Ten grams of fresh leaves of *C. sinensis* were shade dried for 10 days and ground to fine powder using a mixer. One gram of the fine powder was taken and mixed with 50 mL of Milli Q water boiled in a water bath for 20 minutes and allowed to cool. The extracts were filtered using Whatmann No. 1 (pore size 0.2 μm) and mixed with ethanol to precipitate polysaccharides. Centrifugation (Remi RM-12C BL, India) at 8000 rpm for 10min was performed to remove the debris and the supernatant was transferred to a sterile falcon tube and retained for further experiment.

Synthesis of Silver Nanoparticles (AgNPs): In the typical synthesis of silver nanoparticles, 100 mL of silver nitrate (1mM) was prepared using ultrapure water in an Erlenmeyer flask and 2, 4, 6, 8 and 10 mL of aqueous leaf extract was added separately to 90 mL of 1mM silver nitrate solution. The reaction flasks were labelled 1 to 5 for laboratory reference. Control experiment was run without the addition of plant extract to silver nitrate. The flasks including the control were kept in a shaking incubator (CIS-24 Plus, Remi, India) at 37°C in dark condition to reduce photoactivation of silver nitrate. Periodical reduction of silver was analysed at different time intervals with the aid of UV-visible spectroscopy.

Characterization studies: UV-visible spectroscopy remains one of the simple and most reliable techniques for the preliminary characterization of silver reduction. Hitachi U 2900 was employed to determine the maximum absorbance of the reaction mixture (1ml aliquot) in the range of 300 – 700 nm with distilled water as a reference. X-ray diffraction (XRD) analysis was conducted on a Rigaku multiflex diffractometer using monochromatic Cu-K β operated at 40 kV and 100 mA in the diffraction angle 2θ in the range 20 - 80° to study the crystalline nature.

Fourier Transform Infrared spectroscopy (FT-IR) analysis was performed to determine the phytochemical moiety(ies) responsible for reduction of silver. The interaction of functional groups was analysed using FTIR 4200 in the

wavelength range of 4000 – 400 cm^{-1} . Field Emission Scanning Electron Microscopy (FESEM) was employed to explore the surface morphology, shape and dispersive nature of nanoparticles using a 10 KeV Hitachi S-3000H microscope.

Antimicrobial activity of AgNPs– Agar diffusion

method: Antimicrobial susceptibility testing remains one of the tools to evaluate the potency of a drug toward clinical strains. In the susceptibility testing, clinical strains (set A) obtained from PGIBMS and their corresponding antibiotic resistant strains (set B) were used to demonstrate the antimicrobial efficacy of AgNPs¹¹. For screening, log phase bacterial inocula (10^8 cfu/mL) of set A were preferred and optimized using 0.5 McFarland's standard.

The inocula of set A were uniformly spread over MHA plates using a sterile swab (HiMedia™, India). Wells of uniform size (6mm) were made using a sterile cork borer. Silver nanoparticles at a final concentration of 5, 10, 20, 40 μg were added to the wells along with positive and negative controls. Antimicrobial response toward antibiotics, AgNPs and AgNPs-PLGA nanofiber (APN) was determined using set B strains at the pre-defined concentration from screening. Results were interpreted prior to incubation at 37°C for 24 h.

Fabrication of APN membrane: The synthesized AgNPs were immobilized on a PLGA (Poly Lactic-co-Glycolic Acid) nanofibre using an in-house electrospinning device. It consists of an injection spinneret driven by syringe pump with a stainless steel blunt needle (0.5 mm diameter) used to prepare AgNPs-PLGA nanofibre (APN) membrane. The working distance was maintained at 15 cm with the flow rate at 0.05 mL / h. For electrospinning, the applied voltage was 20 kV at 40% relative humidity. APN spun was dried at room temperature and maintained in a desiccator until further use^{12,13}.

Wound healing efficacy of APN membrane: In order to determine the wound healing efficacy of APN membrane, consortia of pathogens (10^8 cfu/mL) isolated from diabetic foot ulcer samples were exposed to the membrane on MHA

medium. The MHA plate was divided into two equal halves. To one half, APN membrane was placed and the other half, PLGA membrane was placed that served as control. Results were analysed after incubation at 37°C for 24h.

Results and Discussion

The reduction reaction was clearly evidenced from the color change when different concentration of extract was added to 1 mM AgNO_3 under shaking condition. At 2-6mL concentrations, the reaction did not last for even 30 minutes that resulted in the precipitation of silver salt. However, at 8 and 10 mL concentrations, the reaction mixture showed typical change in color to brownish yellow within 60 and 30 minutes respectively.

According to the time frame, silver got reduced to silver ions i.e. Ag^+ to Ag^0 when 10 mL of the extract was used which states that the concentration of metabolites (reducing agents) present was sufficient enough to bring about the reduction reaction. Whereas the same could not be achieved when 8 mL concentration of the extract was used as there might be an imbalance between the substrate and reactant concentration^{14, 15}. Control flask showed no change from the initial setup that re-confirmed the involvement of phytochemicals in the reduction process. Moreover, at concentration >10mL of extract, we could observe aggregation in the reaction mixture pertaining to greyish coloration. Thus, the conditions were optimized and AgNPs were synthesized using 10 mL of the extract added to 90 mL of the silver salt (1mM) at physiological pH and 37°C.

The biosynthesis of silver nanoparticles using *C. sinensis* was assessed in a random fashion using UV- visible spectroscopy. One millilitre of sample from each flask (1 to 5) was drawn from the flasks and subjected to spectroscopic analyses at 0, 15, 30, 45, 60 minutes using water as blank. It was only after 15minutes of reaction; we could observe a color change, intensified further at 30th minute and lasted till 60th minute. The optimum concentration of the silver salt getting reduced by the extract was demonstrated from the optical absorption spectral value with a significant peak at λ_{max} 421nm and with a small shoulder peak at around 550nm.

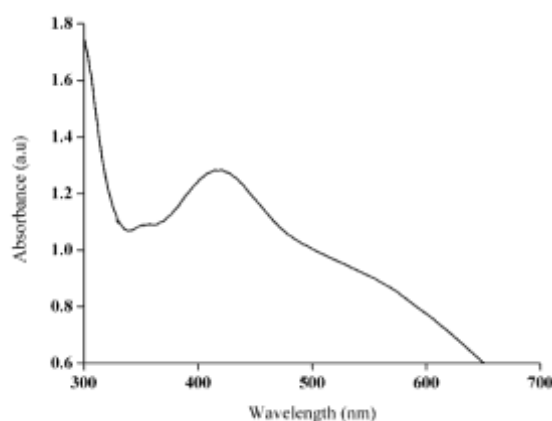


Figure 1: UV-visible spectrum of AgNPs synthesized using *C. sinensis* showing λ_{max} @ 421nm

The absorption depends on the size, shape and the medium surrounding the particle and this sort of spectra clearly attributes to the formation of anisotropic nanoparticles¹⁶,¹⁷. The metal particles were observed to be normal in solution even after a month from their synthesis and remained stable. We mean that there was no observable variation in optical properties of the nanoparticles of the solutions with time.

SEM analysis shows uniformly distributed silver nanoparticles in the surfaces of the cells (Figure 2). The silver nanoparticles were spherical in shape with particle size ranging from 44-76nm. This size based development of nanoparticles using phytochemical moieties was in accordance with earlier reports.¹⁸

FTIR studies were carried out and the representative spectrum of the nanoparticles obtained in our study showed (Figure 3) absorption peak at around 3326.99 cm^{-1} attributing to OH stretching of amides. The peak present at 2926.47 cm^{-1} corresponds to N-H stretch of amines

elucidating the involvement of protein in the reduction. Further peaks at around 1725.93 cm^{-1} , 1434.01 cm^{-1} and 1372.62 cm^{-1} were assigned to C=O stretch, O-H bend of carboxylic acid and phenol. In addition, C-O stretch and C=C bend arising from 1252.41 cm^{-1} , 1092.87 cm^{-1} , 942.45 cm^{-1} and 842.99 cm^{-1} might have resulted due to the surface bound organic molecules involved in reduction thereby conferring stability.

It is ascertained that in the bio-reduction process, Ag^+ ions are trapped due to electrostatic interactions between the silver ions and proteins. Besides reduction, proteins undergo a change in their secondary structure leading to the formation of silver nuclei. In this chain of event, there is a successive growth in the silver nuclei by reduction which gets mounted leading to the formation of AgNPs¹⁹. Alongside, the phytochemical compounds present in the extract viz. ketones, terpenoids, amides, flavones, carboxylic acids and aldehydes as evident from IR spectrum might aid instantaneous reduction of silver to its nanoform^{20,21}.

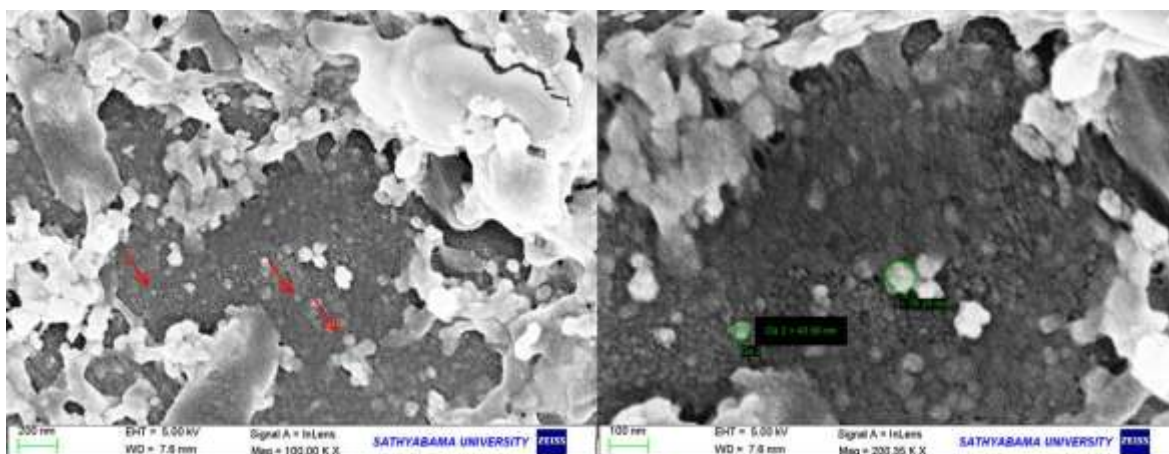


Figure 2: SEM analysis of AgNPs synthesized using *C. sinensis* showing spherical shaped particles at scale bar 200nm and 100nm respectively

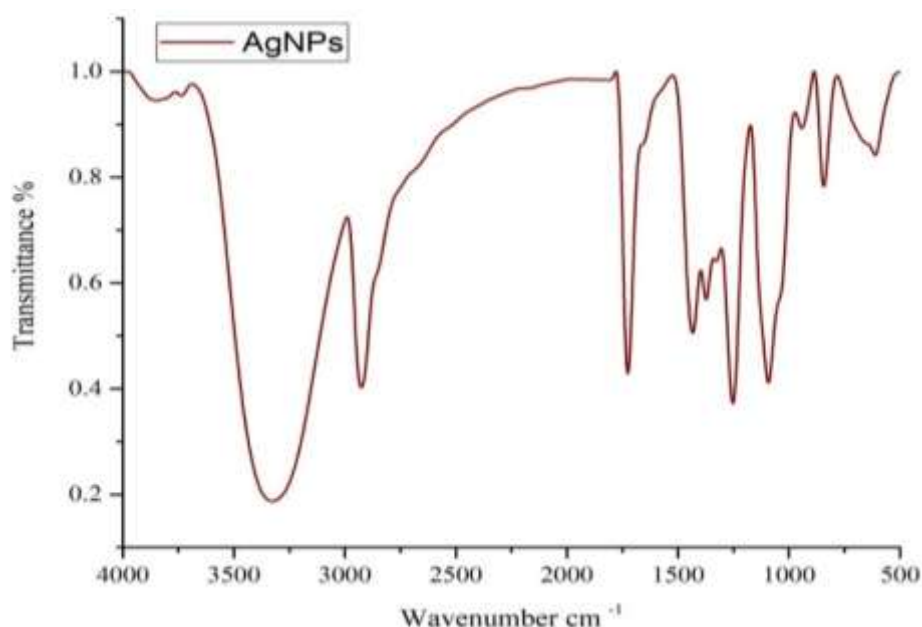


Figure 3: FTIR analysis of green synthesized AgNPs showing the bonding pattern conferring stability

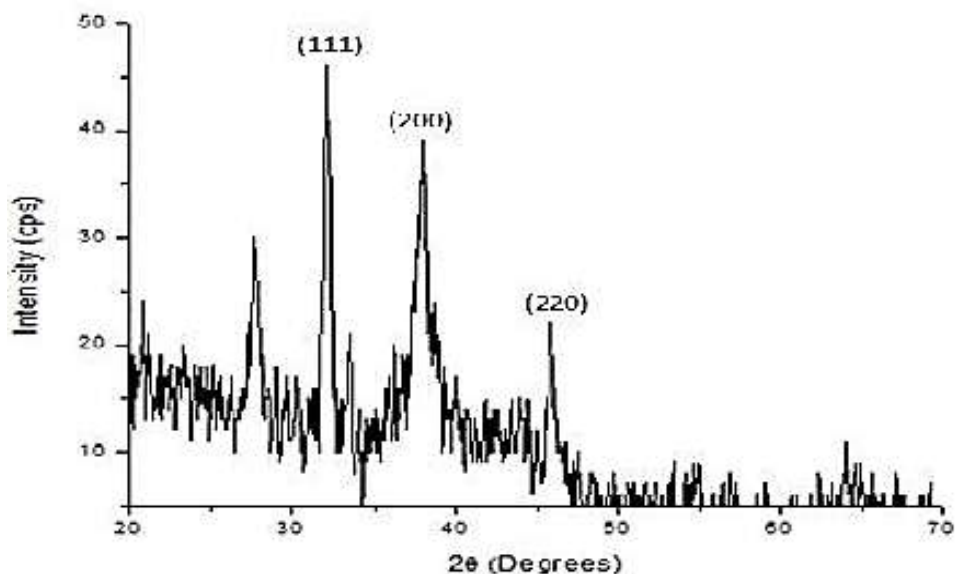


Figure 4: X-ray diffraction pattern of green synthesized AgNPs elucidating the nature of particles

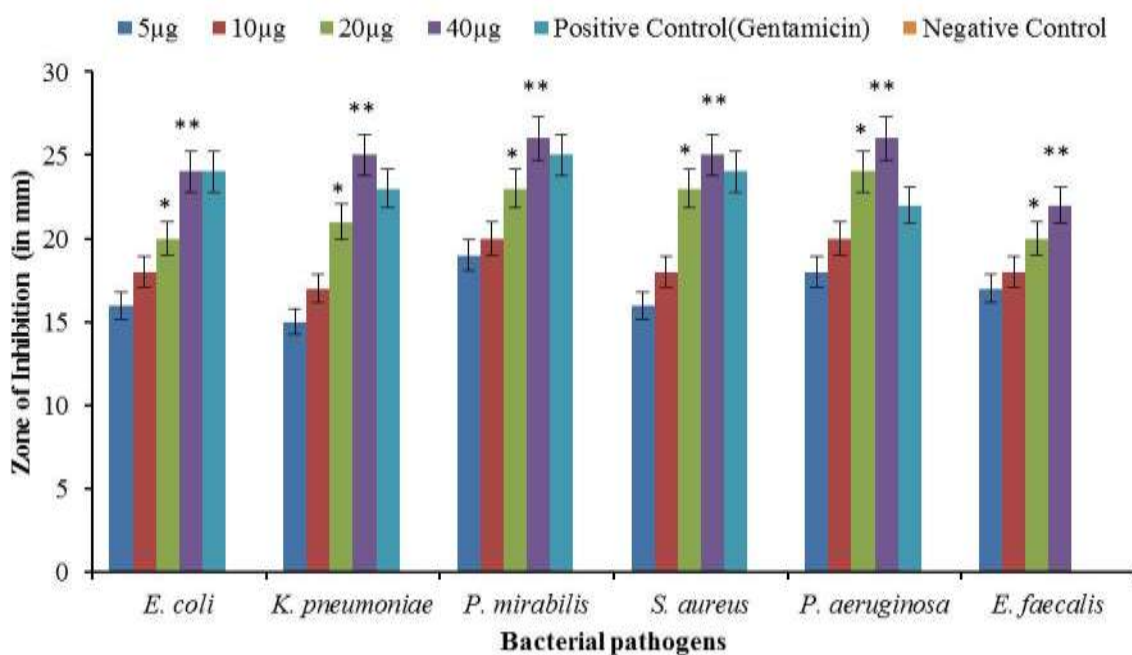


Figure 5: Antibacterial activity of silver nanoparticles toward *E. coli*, *K. pneumoniae*, *P. mirabilis*, *S. aureus*, *P. aeruginosa* and *E. faecalis* at 5, 10, 20 and 40 µg concentrations. Gentamycin (positive control) was used at a concentration of 30µg.

X-ray diffraction is a very important method to characterize the structure of crystalline material used for the lattice parameters analysis of single crystals or the phase, texture or even stress analysis of samples. From XRD analysis (Figure 4), it was confirmed that the AgNPs crystal plane showed 2θ angles at the range of 28.3° , 32.5° , 38.2° , 46.8° corresponding to (210), (112), (111), (231) planes confirming the face-centred cubic symmetry²². Moreover, the mean crystallite size of the developed nanomaterial according to Scherrer's formulae was determined to be ~ 67.8 nm. Silver nanoparticles synthesized from *C. sinensis* were subjected to antimicrobial studies using bacterial clinical isolates (set A;

$n = 6$). AgNPs at a final concentration (5, 10, 20, 40µg) were used to determine the growth inhibition efficacy. There was a significant inhibition in the growth of bacteria at 20µg and 40µg respectively besides other concentrations. It was at higher concentration that the zone size exceeded the standard ZOI measure ($p \leq 0.01$) by 1 – 4mm.

On the other hand, at 50% reduced concentration (20µg), we could appreciate significant zone of inhibition ($p \leq 0.05$) comparable to the lower limit of the standard (gentamycin @ 30µg) at the given concentration. This proves AgNPs as better candidate than antibiotics in bringing about

bactericidal effect at comparatively less concentration as antibiotics. Among the strains tested, *P. mirabilis* was found to be the most susceptible and *E. faecalis* as the most non-responsive strain at all concentrations (Figure 5). This probably relies on the cell wall assembly and membrane architecture of Gram negative and Gram positive strains with the latter possessing a dense, concrete layer of peptidoglycan conferring protection against nanoparticles' intrusion^{23, 24}.

The zone of inhibition is represented as mean \pm SD of the concentration of AgNPs, * 20 μ g fluence standard ZOI ($p \leq 0.05$) and ** 40 μ g fluence maximum standard range ZOI ($p \leq 0.01$).

It has been proposed that antibacterial mechanism of AgNPS was due to generation of Reactive Oxygen Species (ROS) like hydroxyl radicals (OHC). Secondly, the existence of silver ions' affinity toward sulfhydryl groups might bring

about bacterial protein denaturation²⁵. Alongside, the release of silver ions might directly enter into the bacterial cell wall and cause severe damage to the bacteria leading to cell death²⁶. Similar studies have been reported that AgNPs could preferably attack the bacterial respiratory chain and cell division eventually leading to cell death²⁷.

APN membrane developed using electrospinning was observed through electron microscope. SEM results revealed a complete crosslinking of the polymeric fibres (PLGA) like mesh forming pockets to accommodate the nanoseeds (AgNPs) as in figure 6. Alongside, the EDX profile showed elemental composition comprising carbon, silver and trace amount of sodium. The weight % of carbon (60.5%) was found to be the highest which might have its source from coated grids followed by silver (39.15%) and sodium (0.28%). This profile elucidates the successful immobilization of nanoparticles onto membrane (Figure 6).

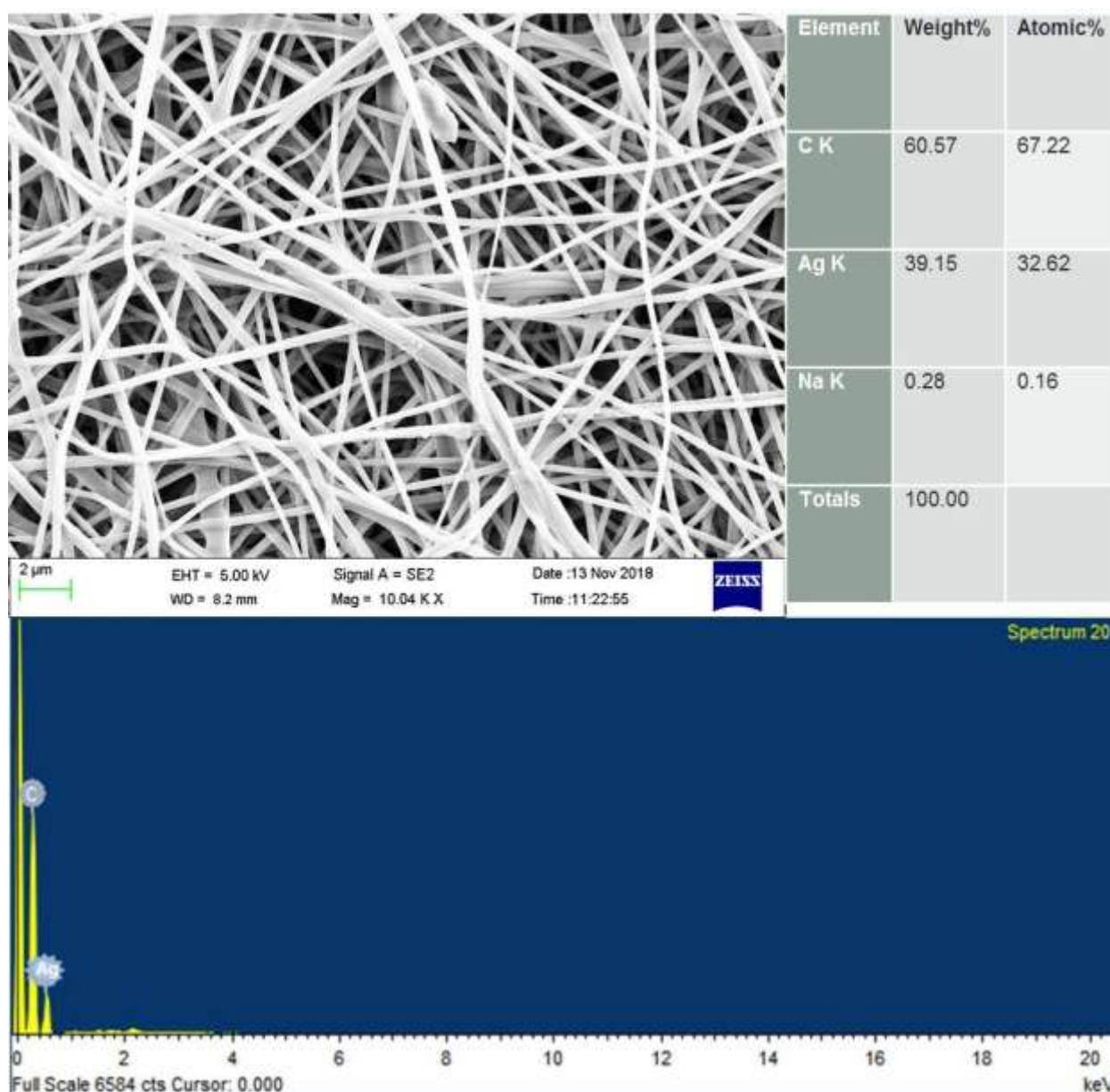


Figure 6: SEM and EDX profile of AgNPs immobilized on APN membrane by electrospinning

Antibiogram screening of antibiotic resistant strains was demonstrated using ESBL strains of *E. coli*, *K. pneumoniae*, *P. mirabilis*, carbapenem resistant *P. aeruginosa* and vancomycin resistant *Enterococci* exposed to different class of antibiotics (Table 1). It was very distinct that these strains did not respond to the antibiotics when compared with the antibiotic sensitivity chart. It was apparent from the zone size that almost all strains remained susceptible towards AgNPs and APN membrane. This proves the potent microbicidal efficacy of AgNPs at a given concentration as the antibiotics. Although different class of antibiotics exhibit different mechanism of action in the containment mission,

microbes could escape the attack using various strategies transforming into resistant strains.

In this microbicidal counterfeit, the main kingpin behind AgNPs mode of action remains obscure. On the other hand, APN membrane exhibited a better biocidal effect synergistic with AgNPs than AgNPs alone ranging from 1 – 9mm. The susceptibility pattern was in the order ESBL resistant strains > Carbapenem resistant strain > MRSA > VRE. This synergistic effect might be due to the assembly of silver ions in close proximity on the membrane enabling easy access to microbial network.

Table 1
The antibiogram profile of multidrug resistant strains (MDR) and their antimicrobial susceptibility toward AgNPs and APN membrane

S.N.	Multidrug resistant (MDR) strains	Zone of inhibition (in mm) for the corresponding antibiotics and NPs at 30µg concentration							
			AMK	CAZ	CRO	GEN	NOR	AgNPs	APN membrane
1	<i>E. coli</i> (ESBL)	S	19-26	25-32	29-35	19-26	28-35	NZ	NZ
		T	12	15	30 ^a	16	19	32	38
2	<i>K. pneumoniae</i> (ESBL)	S	19-26	10-18	16-24	19-26	28-35	NZ	NZ
		T	15	5	23 ^a	24 ^a	15	29	37
3	<i>P. mirabilis</i> (ESBL)	S	19-26	25-32	29-35	19-26	28-35	NZ	NZ
		T	14	20	23	17	30 ^a	30	35
4	<i>S. aureus</i> (MRSA)	S	20-26	16-20	22-28	19-27	17-28	NZ	NZ
		T	13	14	23 ^a	12	14	28	30
5	<i>P. aeruginosa</i> (Carbapenem resistant)	S	18-26	22-29	17-23	17-23	22-29	NZ	NZ
		T	12	16	15	14	21	31	32
Antibiotics for Enterococci			AMP	VAN	ERY	TET	CIP	AgNPs	APN membrane
6	Vancomycin resistant Enterococci (VRE)	S	17	17	23	19	21	NZ	NZ
		T	16	12	10	13	14	25	27

AMK - Amikacin; CAZ - Ceftazidime; CRO - Ceftriaxone; GEN - Gentamycin; NOR - Norfloxacin; AMP - Ampicillin; VAN - Vancomycin; ERY - Erythromycin; TET - Tetracycline; CIP – Ciprofloxacin; NZ – No Zone; APN – AgNPs / PLGA nanofibre; S – Standard Antibiotic zone of inhibition ranges; T – Test strains’ zone of inhibition; ^a*p* < 0.05 which is statistically significant for the zone of inhibition

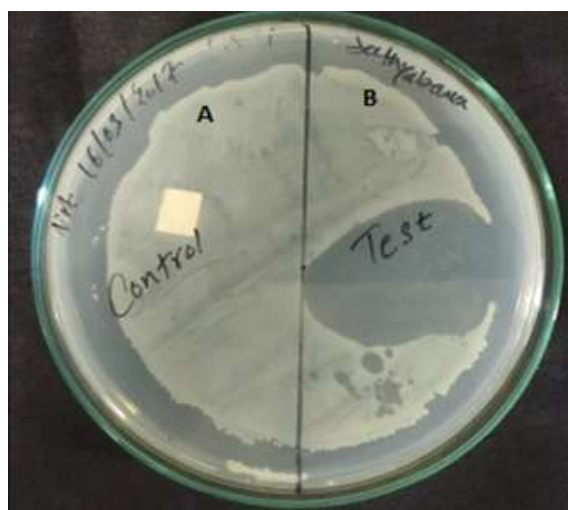


Figure 7: Antimicrobial activity of APN membrane against wound pathogens (A - Control, B – Test)

Further, APN membrane was subjected to antimicrobial susceptibility testing toward bacterial consortia isolated from wound sample. A portion of complete inhibition (~25mm) around the APN membrane was found significant in the bacterial consortia inoculated plates accounting for synergistic effect at 40 µg/mL concentration. Moreover, control (polymer alone) showed no such activity which clearly revealed that the microbicidal action might have advanced through the nanoparticles (Figure 7).

This approach facilitated AgNPs encapsulation and immobilization onto the PLGA membrane that enhanced the probability of metal-microbe interaction attributing to biocidal action. On the contrary, had the nanoparticles had administered as such (colloidal form), the feasibility of aggregation would have increased manifold. Secondly, the particles were trapped inside the nanofibrous membrane which further prevented their leaching into the surrounding medium failing to exhibit its potential. This immobilization approach resolves the purpose of wound dressings wherein targeted delivery of developed nanomaterials can be efficiently conducted provided the *in situ* specificity of the nanoporous fibre is programmed^{28, 29}.

Conclusion

In the present study, AgNPs were synthesized in an eco-friendly mode using *C. sinensis* leaf extract and its antibacterial effect toward human pathogens was determined. The synthesized AgNPs were immobilized in a nanofibre (APN membrane) using electrospinning to evaluate its wound healing efficacy against bacterial consortia isolated from diabetic foot ulcer subjects. Nanocharacteristics were achieved at optimized laboratory conditions.

The purpose of immobilization ensured particle dispersion, enhanced metal-microbe interaction and manifestation of antimicrobial effect to the maximum. Using this immobilization technique, we were able to achieve a better antimicrobial effect at 40µg/mL concentration toward bacterial consortia at par with the individual clinical isolates tested. Such nanoparticle-decorated nanofibres formed by electrospinning offer a scaffold backbone to embed the drug of interest for effective delivery and with great potential where such structures remain mandate while considering the specificity and selectivity parameters in nanomedicine.

Acknowledgement

The authors are grateful to Sathyabama Institute of Science and Technology (Deemed to be University), Saveetha Institute of Medical and Technical Sciences and CSIR – CLRI for funding and providing infrastructural facilities to carry out the research study.

References

1. Freestone I., Meeks N., Sax M. and Higgitt C., The Lycurgus Cup—a Roman nanotechnology, *Gold Bull*, **40(4)**, 270–277 (2007)

2. Chiari G., Giustetto R., Druzik J., Doehne E. and Ricchiardi G., Pre-columbian nanotechnology: reconciling the mysteries of the maya blue pigment, *Appl Phys A*, **90(1)**, 3–7 (2008)
3. Levin A.A., Meyer D.C., Reibold M., Kochmann W., Pätzke N. and Paufler P., Microstructure of a genuine Damascus sabre, *Cryst Res Technol*, **40(9)**, 905–916 (2005)
4. Pal D., Sahu C.K. and Haldar A., Bhasma: the ancient Indian nanomedicine, *J Adv Pharm Technol Res*, **5(1)**, 4 (2014)
5. Pulit-Prociak M., Banach: Silver nanoparticles - a material of the future...?, *Open Chem*, **14(1)**, 76-91 (2016)
6. Amin R., Hwang S. and Park S.H., Nanobiotechnology: an interface between nanotechnology and biotechnology, *Nano*, **6(2)**, 101-111 (2011)
7. Irvani S., Korbekandi H., Mirmohammadi S.V. and Zolfaghari B., Synthesis of silver nanoparticles: chemical, physical and biological methods, *Res Pharm Sci*, **9(6)**, 385-406 (2014)
8. Makarov V.V. et al, Green nanotechnologies: synthesis of metal nanoparticles using plants, *Acta Naturae*, **6(1)**, 35-44 (2014)
9. Ahmed S., Ahmad M., Swami B.L. and Ikram S., A review on plants extract mediated synthesis of silver nanoparticles for antimicrobial applications: a green expertise, *J Adv Res*, **7(1)**, 17-28 (2016)
10. Khan N. and Mukhtar H., Tea and health: studies in humans, *Curr Pharm Des*, **19(34)**, 6141-7 (2013)
11. Bauer A.W., Kirby W.M.M., Sherris J.C. and Turck M., Antibiotic susceptibility testing by a standardized single disk method, *Am J Clin Pathol*, **36**, 493–496 (1966)
12. Li D. and Xia Y., Electrospinning of nanofibres reinventing the wheel, *Adv Biomater*, **16(14)**, 1151-1170 (2004)
13. Guang D.Y., Zhou J., Chatterto N., Li Y., Huang J. and Wang X., Polyacrylonitrile nanofibres coated with silver nanoparticles using a modified coaxial electrospinning process, *Int J Nanomed*, **7**, 5725-5732 (2012)
14. Phanjom P., Zoremi E., Mazumher J., Saha M. and Baruah S.B., Green synthesis of silver nanoparticles using leaf extract of *Myrica esculenta*, *Int J Nano Sci Nanotechnol*, **3(2)**, 73-79 (2012)
15. Priya M., Karunai M., Selvi B. and Paul J., Green synthesis of silver nanoparticles from leaf extract of *Euphorbia hirta* and *Nerium indicum*, *Digest J Nanopart Biostruct*, **6(2)**, 869-877 (2012)
16. Zeinab H., Mohan B., van de Ven Theo G.M. and Nathalie T., One-pot green synthesis of anisotropic silver nanoparticles, *Environ Sci Nano*, **3**, 1259-1264 (2016)
17. Jena B.K., Mishra B.K. and Bohidar S., Synthesis of Branched Ag Nanoflowers Based on a Bioinspired Technique: Their Surface Enhanced Raman Scattering and Antibacterial Activity, *J Phys Chem C*, **113(33)**, 14753–14758 (2009)

18. Ahmed S., Saifullah M., Ahmad B.L. and Swami S., and Ikram: Green synthesis of silver nanoparticles using *Azadirachta indica* aqueous leaf extract, *J Rad Res*, **9(1)**, 1-7 (2016)
19. Li S. et al, Green synthesis of silver nanoparticles using *Capsicum annuum* L. extract, *Green Chem*, **9(8)**, 852 (2007)
20. Pohlit V.F. et al, Plant extracts, isolated phytochemicals and plant-derived agents which are lethal to arthropod vectors of human tropical diseases - a review, *Planta Med*, **77(6)**, 618-630 (2011)
21. Doughari J.H., Phytochemicals: Extraction Methods, Basic Structures and Mode of Action as Potential Chemotherapeutic Agents, In *Phytochemicals – A Global Perspective of Their Role in Nutrition and Health*, Rao Venketeshwer, ed., 1-33 (2012)
22. Rathi Sre, P.R., Reka M., Poovazhagi R., Arul Kumar M. and Murugesan K., Antibacterial and cytotoxic effect of biologically synthesized silver nanoparticles using aqueous root extract of *Erythrina indica* (Lam.), *Spectrochim Acta Part A Mol Biomol Spectrosc*, **135**, 1137-1144 (2015)
23. Jayashree J., Pradhan N., Prasad B., Skull L. and Kumar P., Biosynthesis and Characterization of Silver Nanoparticles using microalga *Chlorococcum humicola* and its antibacterial activity, *Int J Nanomater and Biostruct*, **3**, 1-8 (2012)
24. Sondi I. and Salopek-Sondi B., Silver nanoparticles as antimicrobial agent: a case study on *E. coli* as a model for Gram-negative bacteria, *J. Colloid Interface Sci.*, **275**, 177–182 (2004)
25. Patil R.S., Kokate M.R. and Kolekar S.S., Bioinspired synthesis of highly stabilized silver nanoparticles using *Ocimum tenuiflorum* leaf extract and their antibacterial activity, *Spectrochim Acta Part A Mol Biomol Spectrosc*, **91**, 234-238 (2012)
26. Gomathi M., Rajkumar P.V., Prakasam A. and Ravichandran K., Green synthesis of silver nanoparticles using *Datura stramonium* leaf extract and assessment of their antibacterial activity, *Resour Technol.*, <http://dx.doi.org/10.1016/j.refit.2016.12.005> (2017)
27. Chanda S., Silver nanoparticles (medicinal plants mediated): a new generation of antimicrobials to combat microbial pathogens- a review, In *Microbial Pathogens and Strategies for Combating them: Science, Technology and Education*, Méndez – Vilas A., ed., 1314-1323 (2014)
28. Yang F., Murugan R., Wang S. and Ramakrishna S., Electrospinning of nano/micro scale poly(l-lactic acid) aligned fibers and their potential in neural tissue engineering, *Biomater*, **26(15)**, 2603–2610 (2005)
29. Atiyeh B.S., Costagliola M., Hayek S.N. and Dibo S.A., Effect of silver on burn wound infection control and healing: Review of the literature, *Burns*, **33(2)**, 139-148 (2007).

(Received 25th June 2020, accepted 20th August 2020)